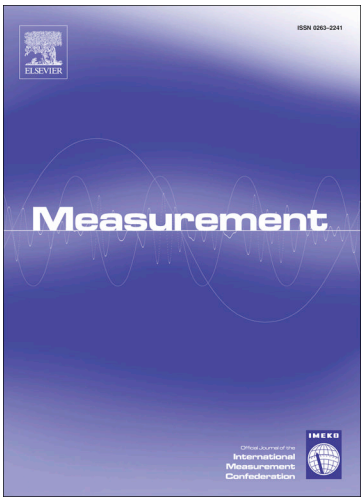

A decision support system for detection of the renal cell cancer in the kidney

Seda Arslan Tuncer, Ahmet Alkan

PII: S0263-2241(18)30277-X
DOI: https://doi.org/10.1016/j.measurement.2018.04.002
Reference: MEASUR 5403

To appear in: *Measurement*

Received Date: 4 November 2017
Revised Date: 29 March 2018
Accepted Date: 1 April 2018

Please cite this article as: S. Arslan Tuncer, A. Alkan, A decision support system for detection of the renal cell cancer in the kidney, *Measurement* (2018), doi: https://doi.org/10.1016/j.measurement.2018.04.002

A DECISION SUPPORT SYSTEM FOR DETECTION OF THE RENAL CELL CANCER IN THE KIDNEY

[1]Seda Arslan Tuncer [2]Ahmet Alkan

[1]Department of Software Engineering, Firat University, Elazig, Turkey.
[2]Department of Electrical & Electronics Engineering, KSU, Kahramanmaras, Turkey.
satuncer@firat.edu.tr, aalkan05@gmail.com

ABSTRACT

Renal cell cancer is the most common type of kidney cancer and usually occurs at an advanced ages. The rapid spread of renal cell cancer and the inability to detect the disease early often results in a fatality. Therefore, it is important to identify the renal abnormalities before the disease reaches the advanced phase. This paper proposes a decision support system that detects renal cell cancer using abdominal images of healthy and renal cell cancer tissues. Renal cell cancer detection involves two main stages as segmentation and cancer detection. In the first step, the kidney areas have been obtained by segmentation based on clustering analysis. In the second step, classification has been made by computer-assisted detection system to identify renal cell cancer. Feature vectors that support the originality of the study at this stage have been created. Subsequently, classification has been made using these feature vectors with the Support Vector Machines (SVMs). For detecting the renal abnormality, 130 different images obtained from the image archiving system of the Radiodiagnostic Department of Fırat University Medical Faculty were used. Thirty of these images have been used to train the K-means classifier. Performance evaluations have been made for both segmentation and classification. In order to measure segmentation success, the Dice coefficient was obtained as 89.3%. Sensitivity, Specificity, Accuracy, Positive Predictive Value (PPV) and Negative Predictive Value (NPV) coefficients, which have been used to determine the classification performance, were obtained as 84%, 92%, 88%, 91.3% and 85.19% respectively.

Keywords: Spinal Cord, Renal cell cancer, Decision support system, K-Means.

1.Introduction

Kidney tumors are either benign or malignant. Simple kidney cysts are the mostly common, a benign mass that is completely different from cancerous tissue. Renal cysts, which often occur as naturally, do not require treatment unless they are causing symptoms [1].

Normally, cells that are the basic building blocks of the body multiply in a controlled manner according to the needs of the body, whereas cancer is the uncontrolled and irregular proliferation of a cell type. Cancer spreads to tissues and organs and invades them [2].

The level of tumor growth in renal cancer is an important indicator of malignancy; renal abnormalities can be correlated with the homogeneity of tissue density for classification [3-6]. Size, growth rate, and heterogeneity or homogeneity of the tumor are important criteria for well targeted tumor treatment [7]. Therefore, the internal status, density, and homogeneity of the lesion are used as parameters in the diagnosis and classification of the lesion. Because manual measurements are time-consuming and exhibit high intra- and inter-operator variability, computer-aided imaging is needed [8,9]. There are many image processing studies on the diagnosis of renal cell cancer. However, segmentation of kidney tumors has rarely been addressed. Studies are mostly focused on segmentation from abdominal images [10-14].

A conventional user-guided, automatic image segmentation method was used to separate right and left kidneys from sagittal images. In that study, 83% success was recorded [15]. In another study, a deformation model represented by statistical information was used on gray scale images. Automatic and manual segmentation showed a similarity of about 86.9% [16]. A computer-assisted detection system was developed using abdominal computed tomography (CT) images of kidney segmentation. The abdominal CT images were digitized and the gray-level threshold method was used for renal segmentation, producing a sensitivity of kidney tumor detection of 85% [17]. A method of automatically performing kidney segmentation of two-dimensional kidney CT images was proposed. In this method, first, the kidney position determination was performed using density based Connected Component Labeling (CCL). This algorithm was applied to tomographic images of different sizes using the kidney and spinal position. Then, kidney segmentation was performed using a growth-based method [18]. A new automatic segmentation method that employs Expectation Maximization (EM) algorithm using tissue information based features is used to identify kidney tumors. The aim in the study was to make a strong distinction by grouping all the pixels between the tumor and the healthy kidney areas. The success of the study was assessed by the kappa factort and about 57% success was obtained [19]. In addition to these studies, there are also knowledge-based models related to adaptive region growing and deformation [20-23]. To extract kidney in abdominal CT scan have been proposed effective approach. Authors have been used template evaluation method and concept of intensity values of a pixel to separate the desired region from the original image [20]. Based on the model of region homogeneity have been developed on a region growing algorithm. The method was successfully tested on artificial images and on CT images [21]. A novel method has been proposed to segment the right and left kidney regions. In this method, segmentation have been implemented using adaptive region growing algorithm by setting the starting point and a threshold value [22]. An automatic region growth method using the properties of the segmented area is proposed. The method was tested for segmentation on test images and of structures in CT and MR images [23].

Apart from these studies, a level set method with shape model has been proposed for image segmentation. In this method, the dimension feature to find the kidneys has been used. The Chan-Vese level set model has been applied to get segmentation. So, the position and the size of the segmented

region have been calculated [24]. An average image account based statistical models have been used extensively in the segmentation of renal cell cancer tissue from abdominal images [25]. A new segmentation method has been proposed which the watershed algorithm based on 2D data to determine renal and lesional densities [26]. In another study, tumor detection was performed using the region growing algorithm considering the homogeneity criterion [27].

In the present study, the anatomical feature of the abdominal region was used to segment the kidneys using the abdominal images. One of the innovations of this study is the separation of the abdominal region into two parts utilizing the spine. Using this method, segmentation has been performed separetely for the right and left kidneys automatically.

The method developed in this study consists of two steps. These are segmentation and tumor detection. Since the success of the first step will directly affect the success of the second stage, the first stage should be examined in detail to segment the kidneys from abdominal images. As a result of segmentation based on K-means, the kidneys are separated from other organs. Thus, the main images for tumor detection are obtained. One of the most interesting points of the present study is the use of both segmented and non-segmented images in the second phase. In total, 100 images were used in the second stage; half of these images have renal cell cancer tissue. Feature extraction was performed on the kidneys segmented in the second stage. In the detection of renal abnormality, the criteria for inferring the feature have been taken into consideration, that have not been previously reported in the literature. In this paper, the use of a minimum number of parameter was aimed at detecting renal abnormalities. These parameters are the right and left kidney areas, and ratios and mean densities for each image. The feature vectors generated for each image were provided as inputs to the classifier, Support Vector Machines. The classification performance for the different parameter values of the support vector machine has been evaluated.

2. MATERIALS

For detecting the renal abnormality, 130 different images obtained from the image archiving system of the Radiodiagnostic Department of Fırat University Medical Faculty were used. Thirty of these images were used for training the classifier, and the others were used for the test procedure. Half of the images used in the test phase were from healthy patients, and the other half were from cancer patients. These images were obtained over the past 10 years. Those images from patients with a disease other than renal cell cancer were excluded from the study. Because kidney cancer is mostly seen above 55 years of age, patients were generally selected to be compatible with this age group. Images are CT images taken at the axial phase after disease opaque material is administered. The images have a cross-sectional thickness of 5 mm and are in DICOM (Digital Imaging and Communications in Medicine) format. The kidney images in the obtained images were manually segmented by a specialist radiologist, and reference images were generated. Figure 1 shows images of abdominal CT images of

healty cells and of renal cell cancer. Figures 1.a, 1.d, and 1.e were obtained from healthy subjects, whereas figure 1.b and 1.c were obtained from from renal cell cancer patients.

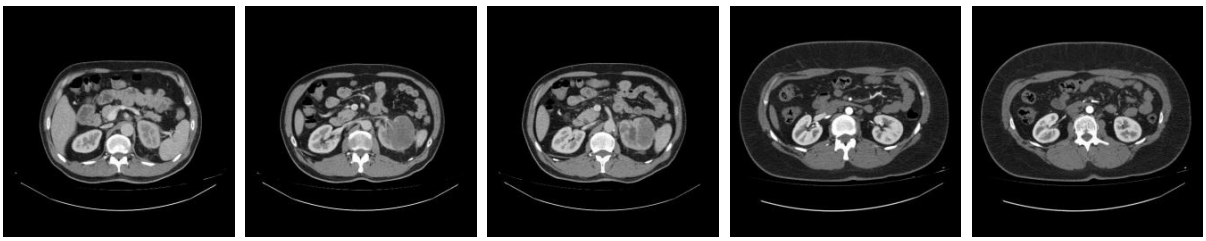

(a) (b) (c) (d) (e)

Figure.1 Sample images of healthy and renal cell cancer patients

3. METHODS

In this paper, the following procedure was followed to segment and classify the kidneys from abdominal images. First, segmentation of the kidney images from other tissues and organs in the abdominal images was performed by K-Means algorithm. This stage also includes pre-processing and post-processing steps that are different from previous approaches. In the second stage, SVM-based classification was used to detect renal cell cancer. Feature extraction was performed on the segmented areas for classification. After the feature extraction process, training data were given as input to the Support Vector Machine. Using that classification, presence or absence of renal cell cancer in the images could be detect. Finally, performance of the K-Means and SVM algorithms were analyzed according to Dice, Accuracy, Sensitivity and Specificity parameters.

Figure 2 shows the flow chart of the procedure. To detail the procedure, the method section is divided into sub-sections of the segmentation and diagnosis support system.

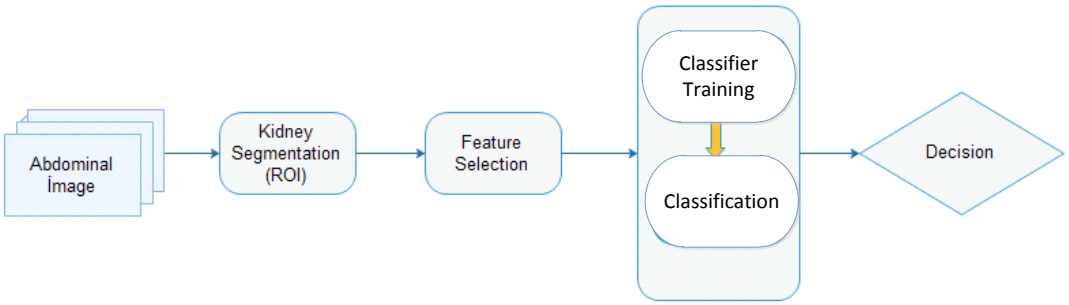

Figure.2 Block diagram of the procedure.

3.1 Segmentation

The first stage is kidney segmentation from the abdominal images. In this stage was used K-means algoritması for segmentation. A clustering analysis method, which is a multivariate statistical technique used to segment data according to similarity and to separate tit into homogeneous subgroups, was applied after the pre-processing phase. K-Means method, which has a non-hierarchical

structure was employed in our clustering analysis [28,29]. The main idea is to define *K* centroids, one for each cluster. A cluster centroid is typically the mean of the points in the cluster. The K-means algorithm works as follows.

a. Select initial centers of the *K* clusters. Repeat steps b through c until the cluster membership stabilizes.
b. Generate a new partition by assigning each data to its closest cluster centers.
c. Compute new cluster centers as the centroids of the clusters [30].

The steps in Figure 3 were performed step by step during the segmentation phase of this study. These steps are pre-processing, clustering analysis and post-processing. After simple morphological procedures in the pre-processing phase, we attempted to reach the kidneys using the spinal cord reference not taken up in previous studies. Figure. 3 (a) shows the original image. Figure. 3 (b) shows the result of segmentation of the spinal cord and its midpoint. All these processes belong to the pre-processing stage. By obtaining the middle point of the spinal cord, the image is divided into two distinct areas where the right and left kidneys are obtained separately. Thus, by clustering analysis, the kidney images can be segmented from the images.

(a) (b) (c) (d) (e) (f)

Figure. 3. Stages of segmentation a) Original image b) Segmented spine and spinal cord c) Scalar multiplication of (a) image with the inverse of (b) image (a.*b) d) Fragmented image e) Segmented right and left kidney f) Merged image

Figure 3(c) is obtained with scalar multiplication of (a) image with the inverse of (b) image (a.*b). It shows the kidney images separately with reference to the midpoint. At this stage, the spinal cord and kidneys in the abdominal image were separated into three different clusters using clustering analysis. Thus, the kidneys have been segmented from other organs. Figure 3 (d) shows the right and left kidney images obtained by segmenting the spinal cord image from these images. In Figure 3.d, other organ fragments are seen with the kidney after clustering analysis. These organs are completely eliminated in the post-processing step. Figure 3.e shows segmented kidneys. Finally, the kidneys were combined and the segmented image was obtained as shown Figure 3 (f).

The Dice coefficient was used to measure the accuracy of segmentation of the kidney. The manually defined and algorithm-generated areas are employed to calculate the Dice coefficient values. This is expressed in equation 1.

$$\text{Dice Similarity Coefficient} = \frac{2*(A \cap M)}{|A|+|M|} \quad (1)$$

In this equation, *A* shows a binary mask of automatically segmented area, and *M* shows a binary mask of the manually segmented area by the doctor. 89.3% average Dice segmentation success was achieved with the above-mentioned process. The segmented kidney images will be used as the input to the diagnostic support system. These steps are of great importance for the success of the classification process.

3.2. The Proposed Decision Support System

The kidneys were segmented and extracted from all images and a new data set was created for the diagnostic support system, where feature extraction is first performed. In fact, feature extraction is a type of size reduction process. Thus, the size of a complex data set is reduced to a simpler form. A properly constructed feature extraction is a factor that affects the success and performance of the diagnostic support system. Another novelty of the present study from other published studies is that a different feature vector is obtained, which is used as an input to the classifier. The process up to now can be expressed as in Figure 4.

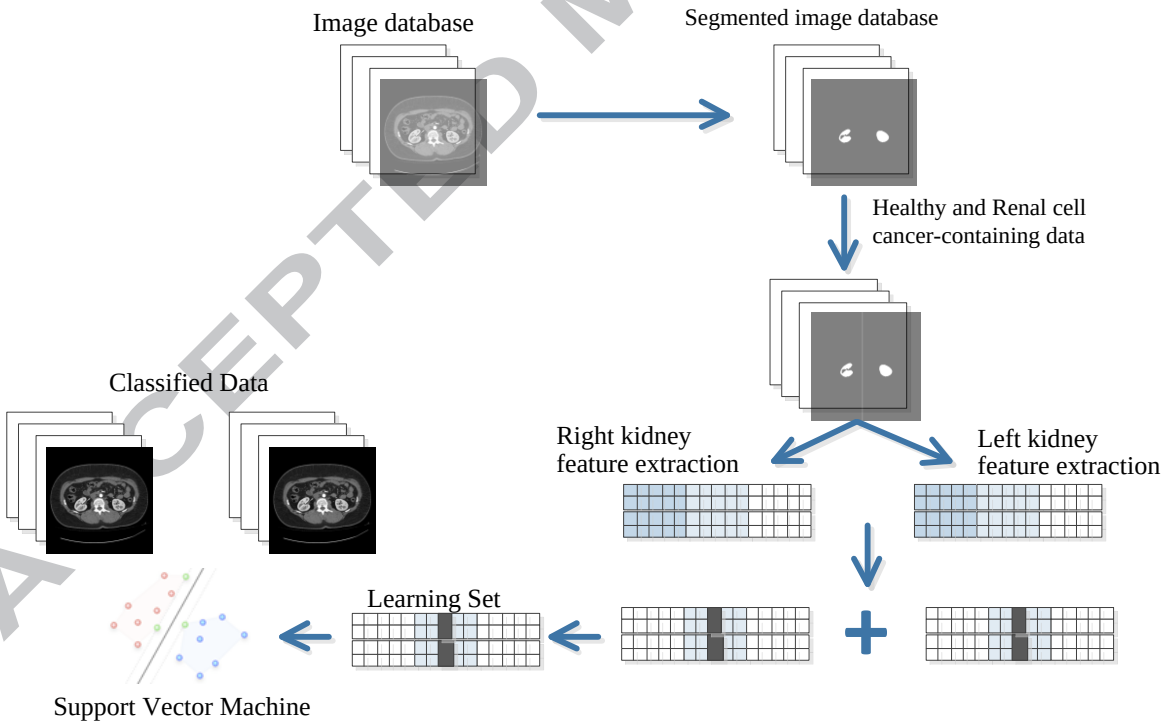

Figure.4 Renal cell cancer detection system

Support Vector Machines were used as the classifier for diagnostic support system. For the Support Vector Machine performance evaluation was performed using different kernel and parameter values.

3.2.1. Feature Extraction

At this stage of the system, previously segmented right and left kidney images are used. As mentioned earlier, a different feature vector have been created in this paper. For this, a total of 4 parameters have been considered. These parameters are total pixel values of the right and left kidneys, mean density values of the right and left kidneys, the areas and density ratios of both kidneys. The reason for choosing these parameters is that they are also used by doctors in the diagnosis of kidney cancer [31]. Abnormal changes in these parameters can be a sign of cancer. These features have not been used in previous diagnostic support system studies. These four properties are given as an input to the classifier. Although there is no sharp measure of the size of the segmented kidneys, the average length is approximately 12 cm and width is 6 cm. In addition, there is no definite ratio of non-healthy kidney sizes because renal cell cancer grows in an uncontrolled manner and changes the size of the kidney. However, uncontrolled growth of both kidney cells at the same time is not a very common occurrence. Equation 2 shows the total number of pixels for a kidney segmented from other images.

$$\text{Total Number of pixels of segmented area} = \sum_{c=0}^{\text{Number of pixel}-1} P_c \tag{2}$$

where the P_C determines whether a pixel in the image is in segmented area or not. *Pc* is 1 for the pixel on segmented area otherwise it is zero. Gray level intensity averages are among the symptoms of cancer because, in the CT image, there is a density difference beetween the renal cell area and the healthy area. The average gray level intensity value is calculated as in Equation 3.

$$\text{Mean gray level density value} = \frac{1}{N}\sum_{(x,y)\epsilon R} a(x,y) \tag{3}$$

where *a(x,y)* is the pixel density at the *x* and *y* coordinates and *N* is the total number of pixel in the segmented area. In the case of uncontrolled proliferation of kidney cells, there are usually differences between the right and left kidney areas. For this reason, the magnitude ratios of the right and left kidneys can also be used as an input to the classifier. Equation 4 shows the proportion of kidney areas.

$$\text{Ratio of right and left kidney areas} = \frac{\sum Pi}{\sum Ki} \tag{4}$$

where P_i and K_i represent the number of pixels of the segmented right and left kidneys, respectively. The fourth parameter is the right and left kidney density ratio as in Equation 5.

$$\text{Density ratio of right and left kidney} = \frac{\sum mi}{\sum ni} \tag{5}$$

where, m_i and n_i show the right and left renal density.

3.2.2 Renal Cell Cancer Classification using the Support Vector Machine

Classification is the process of dividing objects with similar properties into predetermined subgroups. The support vector machine is one of the simplest and most effective methods of classification. The goal is to obtain an optimal separation hyperplane to separate classes [32]. The success of SVM is to

correctly define the hyperplane that can make the most appropriate difference between the two classes. That is, the distance between the support vectors must be maximum.

In this paper, the software MATLAB 'in the BioinformaticsToolbox ™ [12] was used to classify SVM. Figure. 5 shows that inputs of SVMs are the total pixel values of the right and left kidneys, mean density values of the right and left kidneys, area and density ratios of both kidneys. The output is the classification of renal cell cancer and normal images.

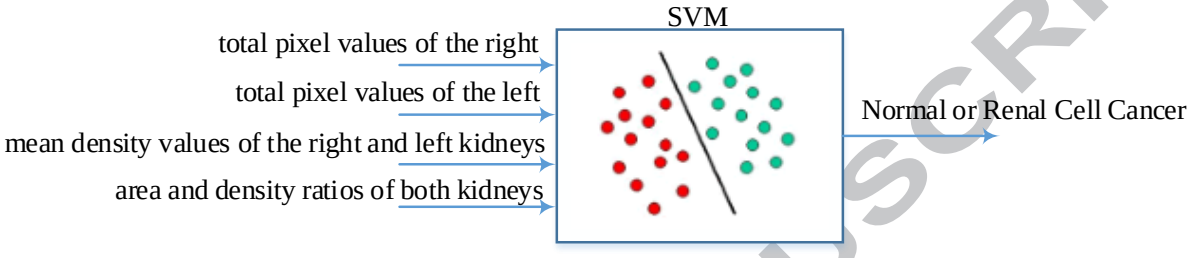

Figure.5 Inputs and outputs of SVM

A total of 30 images were used for SVM training, one-half of which contain renal cell cancer. The selection of the core function plays a critical role in classification with SVM. Radial base, polynomial, linear and sigmoid kernel functions have been tested for the highest classification performance. The highest classification success was achieved with the radial core.

4. Performance Evaluation

Confusion matrix based parameters were used to determine the performance of the diagnostic support system. A confusion matrix is a table frequently used to describe the performance of a classification model (or "classifier") on a set of test data for which the true values are known [33].

Table.1 Confusion matrix

		Actual Value (as confirmed by experiment)	
		Positives	Negatives
Predicted Value (predicted by the test)	Positives	**TP** True Positive	**FP** False Positive
	Negatives	**FN** False Negative	**TN** True Negative

- True Positive (TP) is the number of **correct** predictions that an instance is **positive**.
- True Negative (TN) is the number of **correct** predictions that an instance is **negative**,
- False Positive (FP) is the number of **incorrect** predictions that an instance is **positive**, and
- False Negative (FN) is the number of **incorrect** of predictions that an instance **negative**.

The ratios calculated from a confusion matrix for a binary classifier are as follows.

Sensitivity is the correct calculation rate of healthy people and it’s value is calculated as in Equation 6.

$$\text{Sensitivity} = \frac{\text{TP}}{\text{TP+FN}} \tag{6}$$

Specificity is the correct rate of calculations of renal cell cancers and it's value is calculated as in Equation 7.

$$\text{Specificy} = \frac{\text{TN}}{\text{TN+FP}} \tag{7}$$

Accuracy is the correct detection rate of those with healthy and renal cell cancer and it's value is calculated as in Equation 8.

$$\text{Accuracy} = \frac{\text{TP+TN}}{\text{TP+FP+TN+FN}} \tag{8}$$

Positive and negative predictive values are directly related to the prevalence of the disease in the total images. Positive Predictive Value (PPV) is the percentage of patients with a positive test who actually have the disease. The PPV and NPV are calculated as in Equation 8 and 9. Negative Predictive Value (NPV) is the percentage of patients with a negative test who do not have the disease.

$$\text{PPV} = \frac{\text{TP}}{\text{TP+FP}} \tag{9}$$

$$NPV = \frac{TN}{TN+FN} \tag{10}$$

A total of 100 images were used for the testing stage of the analysis. Half of them were of healthy and the other half were of renal cell cancer patients. Table 2 shows the *TP*, *TN*, *FP*, *FN*, sensitivity, specificity, accuracy, PPV and NPV values obtained as results of classification.

Table.2 Classification results

TN	FN	TP	FP	
46	8	42	4	
Accuracy	Sensitivity	Specificity	PPV	NPV
88%	84%	92%	91.3%	85.19%

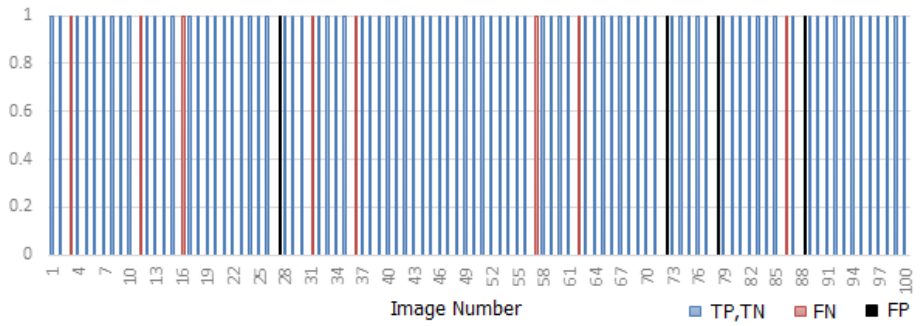

Figure 6. Classification results for each image

Figure 6 shows the performance evaluation of the diagnostic support system. The blue label images shown in Figure. 6 are the sum of *TN* and *TP*. The doctor's decision with the diagnostic support system for a total of 88 images is the same. Red labels (number of *FN*) are images of renal cell cancer.

However, they are images that were determined to be healthy by the decision support system. Black labels were identified as renal cell cancer by the decision support system; however, in reality these images belong to the healthy subjects.

5. CONCLUSION

The first goal of the paper is to automatically perform kidney segmentation on abdominal CT images. The second goal is to detect renal cell cancer tissue from those images. A decision support system has been proposed in this article to achieve the stated objectives. One of the most important features of the decision support system is the specified attribute vectors. To construct the feature vectors, we obtained the attributes after the segmentation of kidneys as the total pixel values of the right and left kidneys, mean density values of the right and left kidneys, and the area and density ratios of both kidneys. Firstly, right and left kidneys were segmented from the images. In the segmentation process, the spinal cord was taken as a reference, unlike in previous studies. For the performance assesment of the proposed segmentation methodology, the Dice criterion was used and average 89.3% segmentation success was achieved. At the end of this process, a second data set (feature vectors) was created from the segmented kidneys for the diagnostic support system. A Support Vector Machine was used for classification of renal cell cancer in the diagnostic support system. The SVM was tested on 100 CT images. Sensitivity, Specificity, Accuracy, PPV and NPV criteria were used for the performance of the decision support system. These values were obtained as 84%, 88%, 92%, 91.3% and 85.19% respectively. The results were checked by the doctor and determined to be reasonable. There are many criteria that influence the performance of the proposed decision support system. The most important and decisive factor of these criteria is to make the correct segmentation. This results are obtained from the presence of many organs on the abdominal images, which makes it difficult to isolate the kidneys. We anticipate that this work will shed light on the future work so that the performance values are higher.

REFERENCES

1. R.J Motzer, N. Agarwal, C. Beard , “Kidney cancer”, Journal of the National Comprehensive Cancer Network, vol. 9 , pp. 960– 977, 2011.
2. E. Ruoslahti, “How cancer spreads”, Scientific American, vol.275, pp. 72–77, 1996.
3. W.G. Bradley, “History of Medical Imaging”, Proceeding of American Philosophical Society, vol.152, pp.349–361, 2008.
4. J. A. Kaufman, J. A. Reekers, J. P. Burnes, A. Al-Kutoubi, C. A. Lewis, B.W. Hardy, S. Kuribayashi, “Global Statement Defining Interventional Radiology”, Journal of Vascular and .Interventional Radiology vol.21 (8), pp. 1147–1149, 2010.
5. H. Singh, J. A. Neutze, "Radiology Fundamentals", Springer Science, https://doi.org/10.1007/978-1-4614-0944-1, 2012.
6. A. Alkan, S.A. Tuncer, M. Gunay, “Comparative MR Image Analysis for Thyroid Nodule Detection and Quantification”, Measurement, vol.47, pp. 861-868, 2014.

7. J.L. Prince, J.M. Links, "Medical Imaging Signals and Systems", Pearson Prentice Hall Bioengineering, New Jersey, USA, pp. 3-13, 2006.
8. M. Marsousi, K. N. Plataniotis, S. Stergiopoulos, "An Automated Approach for Kidney Segmentation in Three-Dimensional Ultrasound Images", IEEE Journal of Biomedical and Health Informatics, Vol.21, pp. 1079 – 1094, 2017.
9. J. R. Bushberg, J. A. Seibert, E. M. Leidholdt, J. M. Bone, "The Essential Physics Of Medical Imaging", Lippincott Williams & Wilkins, Philadelphia, USA ,3,82, 2002.
10. A. Skalski, J. Jakubowski T. Drewniak, "Kidney Tumor Segmentation and Detection on Computed Tomography Data", IEEE International Conference on Imaging Systems and Techniques, pp. 238 – 242, 2016.
11. N. Goceri, E. Goceri, "A Neural Network Based Kidney Segmentation from MR Images", IEEE 14th International Conference on Machine Learning and Applications, pp. 1195 – 1198, 2015.
12. Math Works, MATLAB for Microsoft Windows. Math. Works. Mass., 2018.
13. R. Chav, T. Cresson, G. Chartrand, C. Kauffmann, G. Soulez, J. A. de Guise, "Kidney segmentation from a single prior shape in MRI", 11th IEEE International Symposium on Biomedical Imaging, pp. 818 - 821, 2014.
14. X. Yang, H. Le Minh, T. Cheng, K.H. Sung, W. Liu, "Renal compartment segmentation in DCE-MRI images", Medical image analysis, vol. 32, pp. 269-280, 2016.
15. J. Z. Chen, G. S. Tracton, M. Rao, S. Joshi, E. L. Chaney, S. M. Pizer, "Comparison Of Automatic and Human Segmentation of Kidneys from CT Images", International Journal of Radiation Oncology Biology Physics, vol. 54, pp. 82. 2002.
16. B. Tsagaan, A. Shimizu, H. Kobatake, K. Miyakawa, "An Automated Segmentation Method Of Kidney Using Statistical Information", In Proceeding Medical Image Computing and Computer Assisted Intervention, vol.1, pp. 556–563, 2002.
17. D.T. Lin, C.C. Lei, S.W. Lung, "Computer-Aided Kidney Segmentation on Abdominal CT Images", IEEE Transaction on Information Technology in Bio Medicine, vol. 10, No. 1, 2006.
18. G. Yan, B. Wang, "An Automatic Kidney Segmentation From Abdominal CT Images", IEEE International Conference on Intelligent Computing and Intelligent Systems, vol.1, pp.280-284, 2010.
19. S. Nedevschi, A. Ciurte, G. Mile, "Kidney Ct Image Segmentation Using Multi-Feature Em Algorithm, Based On Gabor Filters", 4th International Conference on Intelligent Computer Communication and Processing, pp. 283,286, 2008.
20. P. Natarajan, B.P. Singh, S. Dwivedi, S. Nancy, "Kidney Segmentation in CT - Scan Image", International Journal of Scientific & Engineering Research, vol:4, pp.221-225, 2013.
21. R. Pohle, K.D. Tönnies, "A New Approach for Model-Based Adaptive Region Growing in Medical Image Analysis", In: SkarbekW, Editor. CAIP, vol. 2124 of Lecture Notes in Computer Science. Springer, pp. 238–246, 2001.
22. D.T. Lin, C.C. Lei, S.Y. Hsiung, "An Efficient Method For Kidney Segmentation On Abdominal CT Images", 8th Australian and New Zealand Intelligent Information Systems Conference, Sydney, Australia, pp. 75-82, 2003
23. R. Pohle, K.D. Toennies, "Segmentation Of Medical Images Using Adaptative Region Growing", Proc. SPIE Medical Imaging, 2(27), pp. 1337-1346, 2001.

24. C.L. Huang, L.Y. Kuo, Y.J. Huang, Y.H. Lin, “Shape-Based Level Set Method For Kidney Segmentation On CT Image”, 22nd Conference on Computer Vision, Graphics, and Image Processing (CVGIP), 2009.
25. H. Park, P.H. Bland, C.R. Meyer, “Construction Of An Abdominal Probabilistic Atlas And Its Application In Segmentation”, IEEE Transactions on Medical Imaging, vol.22(4), pp. 483–492, 2003.
26. R.M. Summers, C.M.L. Agcaoili, M.J. McAuliffe, S.S. Dalal, P.J. Yim, P.L. Choyke, M.M. Walther, W.M. Linehan, “Semi-Automated Segmentation Of Renal Lesions”, Proceedings of International Conference in Image Processing, pp. 293–296, 2001.
27. D.Y. Kim, J. W. Park, “Computer-Aided Detection Of Kidney Tumor On Abdominal Computer Tomography Scans”, Acta Radiologica, vol.45, pp. 791–795, 2004.
28. D. H. Burn, Z. Zrinji, M. Kowalchulk, “Regionalization of Catchments for Regional Flood Frequency Analysis. Journal of Hydrologic Engineering”, Vol.2(2), pp. 76–82, 1997.
29. G-F. Lin, L-H. Chen, “Identification of Homogeneous Regions for Regional Frequency Analysis using the Self-Organizing Map”, Journal of Hydrology, 324, pp. 1-9, 2006.
30. A. Rao, V.V. Srivinas, “Regionalization of Watersheds by Fuzzy Cluster Analysis”. Journal of Hydrology, 318, pp. 57-79, 2006.
31. A. Marhuenda, M.I. Martín, C. Deltoro, J. Santos, J. Rubio Briones, “Radiologic Evaluation of Small Renal Masses (I): Pretreatment Management”. Advances in Urology, 415848, 2008.
32. C. S. Shin, K. I. Kim, M. H. Park, H. J. Kim, “Support Vector Machine-Based Text Detection In Digital Video, Neural Networks for Signal Processing”, X. Proceedings of the 2000 IEEE Signal Processing Society Workshop, Sydney, pp. 634-641, 2000.
33. J. Vilhena, M. R. Martins, H. Vicente, J. M. Grañeda, F. Caldeira, R. Gusmão, J. Neves, “An Integrated Soft Computing Approach to Hughes Syndrome Risk Assessment”, Journal of Medical Systems, vol.41:40, 2017.

Highlights

The proposed decision support system detects renal cell cancer using abdominal images of healthy and renal cell cancer tissues.

Segmentation of kidneys were done using the spinal cord reference not taken up in previous studies.

Renal cell cancer detection involves two stages: segmentation and cancer detection.

Results have shown that using the proposed system for renal cell cancer tissue detection is promising.